Stars and their variability observed from space
C. Neiner, W. W. Weiss, D. Baade, R. E. Griffin, C. C. Lovekin, A. F. J. Moffat (eds)

3D HYDRODYNAMICAL SIMULATIONS OF STELLAR CONVECTION FOR HELIO- AND ASTEROSEISMOLOGY

F. Kupka[1]

Abstract. Hydrodynamical simulations of stellar convection are an essential theoretical tool for gaining insight into the physics of mixing and heat transport by convection, and also into the interaction of convection with pulsation. They are particularly useful for obtaining an accurate description of the structure of the superadiabatic layer, which is important to explain the observed frequencies of p-modes in solar-like oscillating stars. The simulations can also be used to probe analytical models of excitation and damping of modes, and thus explain their amplitudes, and eventually the physical completeness of such models. This presentation discussed general challenges of such 3D hydrodynamical simulations developed for helio- and asteroseismology; it summarized some recent results in this field for the Sun, and which are also relevant to other lower main-sequence stars.

Keywords: convection, hydrodynamics, asteroseismology, turbulence, methods: numerical

1 Introduction

Convective instability in a gravitationally stratified fluid can be derived from considering small vertical perturbations of a fluid element. If adiabatic expansion results in a density ρ_1 of the displaced fluid that is less than the density ρ_2 of its new local environment, the fluid is convectively unstable. Equivalent criteria are those of superadiabaticity ($\nabla > \nabla_{\mathrm{ad}}$), or an entropy gradient dropping against the direction of gravitational acceleration (cf. also Kupka & Muthsam 2017). Such an unstable stratification triggers the generation of velocity fields. Those are described by conservation laws (the Navier-Stokes equation, NSE) which enable predictions of heat transport in a fluid, mixing of a fluid, the coupling of convection to pulsation and shear flows, and (since stellar fluids are actually plasmas) their interactions with magnetic fields including, dynamo effects.

Numerical approximations to solutions of the fully compressible Navier-Stokes equation form a powerful tool to model convective flows in stars, and their interactions with various physical processes. If the surface layers are included in such numerical models, radiative transfer has to be accounted for (i.e., *radiation hydrodynamical (RHD) simulations*). They have been developed continuously for the last 40 years or so (cf. Nordlund 1982; for reviews and further references see also Nordlund et al. 2009 and Kupka & Muthsam 2017). *Magnetohydrodynamics (MHD)* (cf. Galtier ???? and Brun & Browning 2017 for reviews and references) and radiation magnetohydrodynamics (RMHD) (see, for instance, Stein 2012) are based on effectively the same physical and numerical concepts, but include magnetic fields generated by, and interacting with, the stellar plasma of the simulation models.

The following considers the non-magnetic case. RHD are now mainly performed for the case of three spatial dimensions (3D), although the case of two dimensions (2D) still has applications where 3D simulations have remained unaffordable. The basic numerical equations of (radiation) hydrodynamics are recalled in Sect. 2, which sets the stage for applications to helio- and asteroseismology. Three important simulation scenarios, plus the methodological limitations of the RHD simulation approach, are summarized in Sect. 3. Further recent results on the damping of solar p-modes by RHD simulations are described in Sect. 4. Conclusions are summarized in Sect. 5.

2 Numerical (radiation) hydrodynamics and its applications to helio- and asteroseismology

Supplemented by the continuity (mass conservation) and energy equation, the *Navier-Stokes equation* in a gravitational field with acceleration $\boldsymbol{g}$ and with radiation but without a magnetic field, reads

$$\partial_t \rho + \mathrm{div}\,(\rho \boldsymbol{u}) = 0, \tag{2.1}$$

[1] MPI for Solar System Research, Justus-von-Liebig-Weg 3, 37077 Göttingen, Germany

$$\partial_t(\rho \boldsymbol{u}) + \mathrm{div}\,(\rho(\boldsymbol{u}\otimes\boldsymbol{u})) = -\mathrm{grad}\,p + \mathrm{div}\,\boldsymbol{\pi} + \rho\,\boldsymbol{g}\,, \tag{2.2}$$

$$\partial_t\,(\rho E) + \mathrm{div}\,((\rho E + p)\,\boldsymbol{u}) = \mathrm{div}(\boldsymbol{\pi}\boldsymbol{u}) - \mathrm{div}\,\boldsymbol{f}_{\mathrm{rad}} - \mathrm{div}\,\boldsymbol{h} + \rho\boldsymbol{u}\cdot\boldsymbol{g} + q_{\mathrm{nuc}}. \tag{2.3}$$

In addition to density ρ, velocity $\boldsymbol{u}$, gas pressure p and viscous stress tensor $\boldsymbol{\pi}$, the energy equation invokes the conductive heat flux $\boldsymbol{h}$ and the nuclear energy generation rate q_{nuc}, but for *stellar envelopes* both these last two can be neglected. Assuming the radiation field to be sufficiently isotropic, the pressure p is usually considered to represent the sum of the gas pressure and the radiative pressure.

At large optical depths the diffusion approximation of radiative transfer holds:

$$\boldsymbol{f}_{\mathrm{rad}} = -K_{\mathrm{rad}}\,\mathrm{grad}\,T. \tag{2.4}$$

Here, $T = T(\rho, \varepsilon, \text{chemical composition})$ is the temperature, $E = \varepsilon + \frac{1}{2}|\boldsymbol{u}|^2$ is the total specific energy without gravitational potential energy, ε is the specific internal energy, and K_{rad} is the *radiative conductivity*,

$$K_{\mathrm{rad}} = \frac{4\mathrm{ac}T^3}{3\kappa\rho} = \frac{16\sigma T^3}{3\kappa\rho}, \tag{2.5}$$

with $\kappa = \kappa_{\mathrm{Ross}}(\rho, \varepsilon, \text{chemical composition})$ denoting the Rosseland opacity.

In stellar physics $\boldsymbol{\pi} \approx 0$ as $\nu \ll \chi$, where ν is the kinematic viscosity and χ the radiative heat diffusivity. It is replaced by a *sub-grid scale viscosity* (physical model of numerically unresolved scales, which is commonly associated with the term *large eddy simulations* or *LES*), *artificial viscosity* (numerical scheme stabilizing simulations), or through *numerical viscosity* from the discretization of advection (terms such as $\mathrm{div}\rho(\boldsymbol{u}\otimes\boldsymbol{u})$), as occurs in *implicit large-eddy simulations* or *iLES*.

In *optically thin layers* the radiative flux is computed by integrating the stationary limit of the radiative-transfer equation for the intensity I_ν:

$$\mathbf{r}\cdot\nabla I_\nu = \rho\kappa_\nu(S_\nu - I_\nu). \tag{2.6}$$

Here, S_ν is the source function. Summations over bins of frequency averages assure affordability of *non-grey radiative transfer* (4 to 12 bins are common). Owing to resource constraints, this is done in *local thermal equilibrium, LTE*: $S_\nu = B_\nu$ (the Planck function), with non-LTE effects accounted for only very approximatively, if at all.

Angular integration to compute div $\boldsymbol{f}_{\mathrm{rad}}$ is performed by integrating over a (necessarily heavily undersampled) set of rays (as done in most such codes), or by a truncated moment expansion approach (such as the 3D Eddington approximation by Unno & Spiegel (1966) to yield:

$$J_\nu = \frac{1}{4\pi}\int I_\nu(\mathbf{r})d\omega, \qquad \text{and} \tag{2.7}$$

$$q_{\mathrm{rad}} = -\mathrm{div}\,\boldsymbol{f}_{\mathrm{rad}} = 4\pi\rho\int_\nu \kappa_\nu(J_\nu - B_\nu)d\nu. \tag{2.8}$$

To complete the setup of a numerical simulation, the physical problem has to be defined. To that end, the microphysical properties are specified by an equation of state and opacity data, usually given in tabulated form. The chemical composition of the fluid has to be defined, and because a numerical simulation can only account for a finite spatial domain, the latter has to be constructed by choosing a specific volume and the local spatial resolution. Initial conditions are often taken from a 1D model. The environment of this domain is specified through boundary conditions, which may either be open (to allow for inflow and outflow of fluid), closed (to allow only for inflow and outflow of energy), or periodic (usually in horizontal directions). The evolution of this system with time is performed to find a statistically quasi-stationary state. This relies on a quasi-ergodic hypothesis which enables computing ensemble averages from time averages to describe the system through its basic statistical properties. This is also useful for comparisons with 1D models.

The choice of a particular discretization approach requires specifying the numerical grid and its associated coordinate system (Cartesian, polar/spherical/cylindrical, mapped or irregular), the discretization of various terms in the underlying hydrodynamical equations (conservative or non-conservative with respect to mass, momentum and energy, specification of dissipation at small scales and subgrid scale physics), the method of time integration (explicit or (semi)-implicit, multi-stage or multi-step, etc.), and whether the grid values are considered to be interpolated (as in a finite difference method) or volume averages (as in a finite volume approach).

The following applications of 3D RHD of stellar convection are of particular interest in the context of helio- and asteroseismology. First, 1D stellar models can be calibrated, based on data obtained from 3D RHD. This can improve models of convective stellar envelopes and atmospheres (e.g. Magic et al. 2015; Tanner et al. 2016). Secondly, more realistic mean structures can be derived from the RHD simulations for the (near) surface layers of stars. To that end the 3D model is averaged to compute a new mean structure. The latter can be "patched" on top of 1D stellar structure and stellar evolution models. The new 1D model obtained this way can be used for further research. This procedure has been used, for example to study near surface effects of convection on solar-like oscillations in stars (Rosenthal et al. 1999; Sonoi et al. 2015). Finally, quantities of interest can be evaluated directly from the 3D RHD simulation. This approach is of particular interest in the study of mode excitation and mode damping (Stein & Nordlund 2001; Belkacem et al. 2019; Yixiao et al. 2019).

3 Simulation scenarios and methodological limitations

Surface convection zones in main-sequence stars and white dwarfs can be studied with 3D RHD simulations performed for the box-in-a-star scenario. This is based upon the fact that, for those stars, the surface pressure scale-height $P/(\rho\, g) = H_p \ll R$, where R is the stellar radius. Hence, the curvature of mass shells along the radius of such a star, which supposedly rotates slowly enough to be roughly spherically symmetric, is small along a vertical extent of 10 to 12 pressure scale-heights centred around the stellar surface. Cartesian box geometry with a constant vertical gravitational acceleration then allows a good approximation for a set of mass shells along the stellar radius. The horizontal extent of such a simulation box is chosen to be large enough so that near the bottom of the box, where H_p and thus convective flow structures are largest, periodic boundary conditions in the lateral directions do not constrain constrain the flow significantly. In this case structural sizes, such as the width of granules at the stellar surface, are not influenced by introducing this simulation geometry.

The 3D RHD simulations provide numerical solutions for this scenario on a grid in space and time. That enables us to compute mean structures and perform a patching of the averaged 3D structure on top of a 1D stellar structure model. Using an earlier version of the STAGGER code (see also Magic et al. 2015) Rosenthal et al. (1999) demonstrated that the differences in frequencies between solar observations and 1D models such as the famous "model S" by Christensen-Dalsgaard et al. (1996) can partially be explained by effects not accounted for in the standard 1D models: turbulent pressure and radiative cooling in a horizontally inhomogeneous medium. That explains the *structural part of the near surface effect*, the discrepancy between observed and predicted p-mode frequencies at high radial order, n. Using a grid of numerical simulations constructed with the CO5BOLD code Sonoi et al. (2015) studied the dependency of this structural near-surface effect for various stellar spectral types (F to K for main-sequence stars and the lower part of the red giant branch). They noticed a significant variation of the effect with T_{eff} and $\log(g)$. It was confirmed by Ball et al. (2016), who used the MuRAM code for F–K main-sequence stars and also included effects on low-degree non-radial modes (ℓ of up to 3) in their analysis. For a summary of the contributions that appear in addition to these structural effects, i.e. the so called *modal effects*, the review by Houdek & Dupret (2015) provides further insights (and are also a topic in the presentations by G. Houdek [PAGE] and J. Schou [PAGE]). Online resources using the patching of 3D RHD simulations can be found at a webpage on the TOP tool, a Python library for asteroseismology published by Reese, Ballot & Putigny at `https://top-devel.github.io/top/index.html`, with examples given at `https://top-devel.github.io/top/examples.html#surface` based on the ANTARES code (Muthsam et al. 2010; see also Belkacem et al. 2019).

Apart from investigating structural effects upon p-mode frequencies, 3D RHD can also be used to study the near-surface part of the eigenfunctions of high-order radial p-modes. The restriction to high radial order is caused by the slow decay of eigenfunction amplitudes and their contributions inside the star for lower-order modes and the large computational costs of deep 3D RHD simulations with sufficient spatial resolution, thermal relaxation, and long statistical sampling times for resolving p-mode damping and computing work integrals.

For the Sun, that implies $n \gtrsim 15$ (or perhaps somewhat less), $n \gtrsim 7$ (or perhaps a bit larger) for late Am/Fm stars, and $n \gtrsim 50$ for DA white dwarfs with $T_{\text{eff}} \sim 12000\,\text{K}$, (note the latter have not been detected yet in stars). The study of vertical eigenmodes in RHD simulations of the solar surface has been pioneered by Stein & Nordlund (2001), who compared the properties of such modes with the upper part of radial eigenmodes derived from full solar-structure 1D models, which requires scaling of mode amplitudes for reasons explained in further detail by Belkacem et al. (2019).

Alternatively, one can compute work integrals directly from the RHD simulations. Antoci et al. (2014) and Smalley et al. (2017) have demonstrated that an accurate calculation of the turbulent pressure contributions to the work integral is key to understanding which modes are excited in cool Am and Fm stars. This is particularly challenging for 1D models, as they have to be based on a non-local model of convection. For 3D RHD simulations of such objects one would have to ensure that the damping and driving regions of intrinsically unstable modes (e.g., for $n \gtrsim 4$) fit (mostly) into the box to allow reliable work integral computations (especially for $n \gtrsim 7$ in the cases discussed in those papers). Otherwise, polar geometry and deeper domains would be needed, and would lead to even higher computational costs.

Not all the box modes present in 3D RHD are actually observable in stars. An example is p-modes of DA white dwarfs with shallow convection zones and effective temperatures close to 12000 K, where the equivalent of high radial order p-modes are clearly visible in the numerical simulations (cf. Kupka et al. 2018) though no observations have been reported yet. This is due partlyto the technical challenge of detecting modes in the 4 Hz region for faint stars. and partly to the fact that the amplitudes in the simulation boxes are related to their much smaller mode masses which they have, compared to those of full stellar structures.

To study the interaction of envelope convection zones with low radial-order modes, such as in the case of classical variables, much larger fractions of the stellar volume have to be accounted for. This motivates the use of polar coordinates and simulation boxes that may be called "wedge-in-a-star" (having a fixed azimuthal and/or polar opening angle and laterally periodic boundary conditions), "annulus-in-a-star"(covering all azimuthal angles in 2D), or a "spherical shell-in-a-star" (the 3D counterpart of the former). Global 2D simulations (in "annulus-in-a-star" geometry) of the fundamental mode of a Cepheid and its interaction with the mode-driving convection zone due to ionization of He II have been described by Kupka et al. (2014) with a simulation featuring more than 13000 azimuthal zones. They also support the study of non-radial modes (or, in 2D, their counterparts in cylindrical geometry). The key challenges of such multi-dimensional RHD calculations are the computational costs of a sufficiently high spatial resolution near the surface, and the necessity of a long relaxation time. (The drastic effects of insufficient resolution have been demonstrated by Mundprecht et al. 2013 for a "wedge-in-a-star" simulation of the same object).

It may be tempting to demand global simulations of stars to derive results for the damping of p-modes in solar-like stars or for the main radial modes of classical variables and their interaction with convection or higher-order modes. However, for the case of solar-like stars this is not feasible with present, semi-conductor based technology, as was demonstrated by Kupka & Muthsam (2017) (their Table 2). Such a calculation, at a resolution comparable to that of Belkacem et al. (2019), requires 3×10^6 times more grid points than the former (with a 400 times larger area at the same resolution and a 20 times deeper simulation domain, even with highly adapted spatial grids) and a 5000 times longer integration time (to resolve the solar modes, an integration time similar to the observing time of SOHO can be expected), which results in a computational demand that is more than 10^{10} times greater than the simulations used by Belkacem et al. (2019) and Yixiao et al. (2019), and is several orders of magnitude beyond what we can expect from exascale computers during the next 10 years. Likewise, while an in-depth study of classical variables with 2D RHD for a full annulus has now become feasible, 3D RHD of just a single star of this class will either be severely restricted in integration time, or in resolution, or in both, even if the exascale supercomputers of the next decade were to be used with highly optimized simulation codes.

4 Some recent results on solar p-modes

Recent 3D RHD simulations of the convective surface of the Sun have supported detailed analyses of p-mode damping processes. The simulations have aimed at characterizing the main damping contributions by various physical mechanisms (Belkacem et al. 2019) and at computing the theoretical oscillation amplitude and frequency of maximum power $\nu_{\max}$ (Yixiao et al. 2019), among others. Fig. 1 compares the spectral power of the vertical mean velocity evaluated for the layer where the mean temperature equals the (solar) effective temperature, for two 3D RHD simulation runs with ANTARES. The first one, called cosc13, has been published by Belkacem et al. (2019); the latter, called wide4, has been analyzed in==by Leitner et al. (2017) and Lemmerer et al. (2017). Both simulations have the same resolution (11.1 km vertically, 35.3 km horizontally), the same element abundances, opacity tables and starting model, and are based on a 4-bin averaged non-grey radiative transfer with distinct rays for angular integration (see Belkacem et al. 2019 for details). Limited by the sound speed in deep layers and shock waves near the top, and a Courant number associated with the numerical methods used, the time steps are usually less than 0.2 sec.

However, the two simulations differ in several aspects. Wide4 has a 570 km deeper simulation box, i.e., its total vertical extent is 4.45 Mm compared to the 3.88 Mm of cosc13; it also ranges 600 km further into the quasi-adiabatic part of the convection zone. This explains why the three box vertical p-modes (fundamental one with no node in the interior at the lowest frequency, and the first and second overtones with one and two interior nodes, respectively) appear at lower frequency in the simulation wide4 compared to cosc13. In an analysis they thus have to be compared to different solar radial p-modes (see Belkacem et al. 2019 for details). The

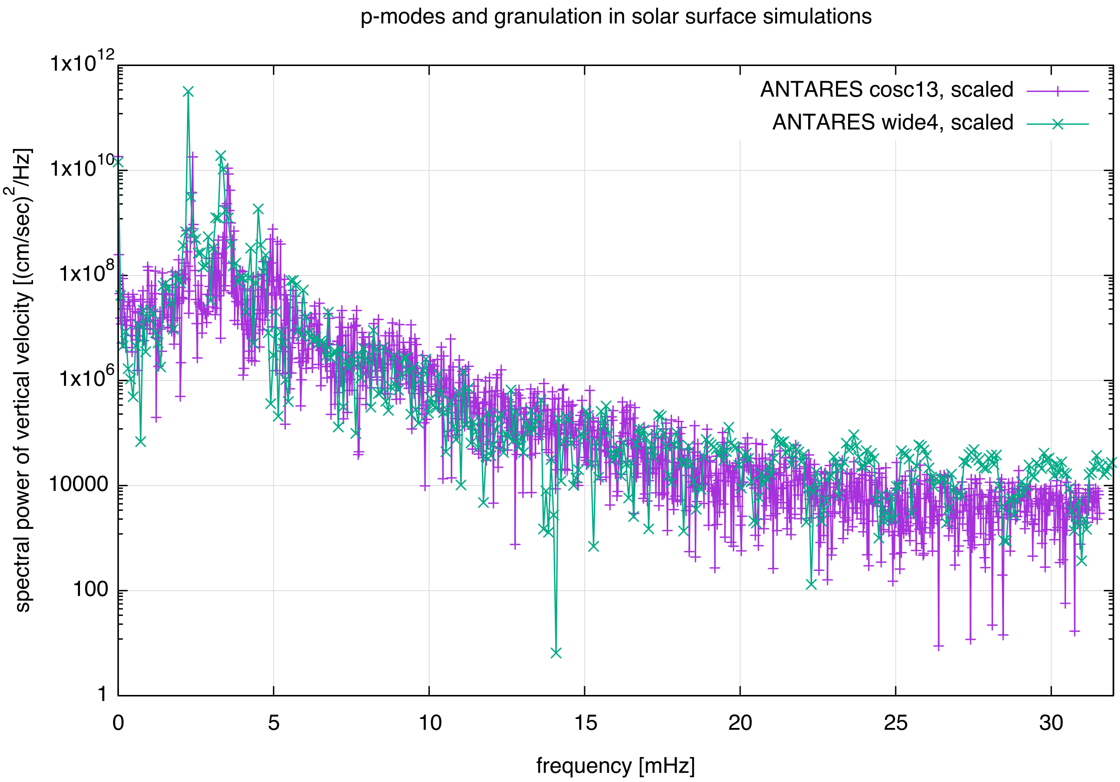

Fig. 1. Spectral power of velocity for two solar granulation simulations performed with ANTARES, evaluated for the layer where the mean temperature equals the (solar) effective temperature. Scaling is necessary to account for the different areas and averaging times of both simulations, but here it was actually set such that both data sets agree in the region from 1–2 mHz with the results obtained by Yixiao et al. (2019) (not shown in the figure).

difference in data output rate (8.54 sec for wide4 and 15.84 sec for cosc13) is less important, as it corresponds to frequencies 100 times smaller than those associated with the simulation time steps, but 10 times larger than the mode frequencies. Fig. 1 therefore truncates the spectrum at about the Nyquist frequency of the lower sampled simulation. The difference in horizontal extent of the simulation domain (18 Mm for wide4 compared to 6 Mm for cosc13) should actually lead to smaller mode power for the simulation with the larger horizontal area (Belkacem et al. 2019). However, the sampling time of wide4 is only 12420 sec (about 3.5 hrs) instead of 40012 sec (about 11 hrs) used for cosc13. Thus, whereas the second mode around 3.5 mHz is resolved in cosc13 (the first one at 2.4 mHz is not), neither is resolved in the case of wide4. The amplitudes obtained are therefore not yet reliable, and the simulation would have to be continued for a longer period of time to obtain more accurate information. between several days and one week of stellar sampling time is necessary to resolve all three modes reliably.

The main conclusion from the study of (Belkacem et al. 2019) has been that, at least for the mode near 3.5 mHz, the different contributions associated with fluctuations of the gas pressure (induced by perturbations of the radiative and enthalpy flux as well as the dissipation rate of turbulent kinetic energy ϵ) can partially cancel each other while being comparable to effects caused by perturbations of the turbulent pressure. In particular, ϵ plays a role that is equally important for the amplitudes of p-modes in the Sun as the other three contributions.

5 Conclusions

The existing simulations used for studying p-modes in solar-like stars are already a very useful tool for gaining insights into the physics of mode amplitudes in addition to mode frequencies. To proceed further, such simulations should be conducted over longer time-scales (a week or a few weeks of solar/stellar time)q at a sufficiently high sampling rate, if the granulation background spectrum should also be investigated with the same numerical data. The influence of boundary conditions, box sizes, and spatial resolution will have to be considered in more detail, and a comparison of simulations based on different discretization methods will be necessary to ensure that the dissipation rate of turbulent kinetic energy is calculated reliably. Evidently, it will be highly informative – and also for gaining a theoretical understanding of the scaling laws used in asteroseismology – to repeat such studies for stars other than the Sun. The main limitation of this approach is the excessive amount of computing resources it requires: simulations have to be planned carefully, to obtain the desired results within an affordable amount of computing time and to avoid unrealistic demands on supercomputing power presently available or during the next decade.

The author gratefully acknowledges partial support through the Austrian Science Fund (FWF) project P29172-N27, and the European Research Council Synergy Grant WHOLE SUN #810218.

References

Antoci, V., Cunha, M., Houdek, G., et al. 2014, ApJ, 796, 118 (8 pp.)

Ball, W. H., Beeck, B., Cameron, R. H., & Gizon, L. 2016, A&A, 592, A159 (8 pp.)

Belkacem, K., Kupka, F., Samadi, R., & Grimm-Strele, H. 2019, A&A, 625, A20 (15 pp.)

Brun, A. & Browning, M. 2017, Living Reviews in Solar Physics, 14:4, 133 pages

Christensen-Dalsgaard, J., Dappen, W., Ajukov, S. V., et al. 1996, Science, 272, 1286

Galtier, S. ???? (Cambridge University Press, Title = Introduction to Modern Magnetohydrodynamics, Year = 2016)

Houdek, G. & Dupret, M.-A. 2015, Living Reviews in Solar Physics, 12:8, 88 pages

Kupka, F., Mundprecht, E., & Muthsam, H. J. 2014, in IAU Symposium, Vol. 301, Precision Asteroseismology, ed. J. A. Guzik, W. J. Chaplin, G. Handler, & A. Pigulski, 177–184

Kupka, F. & Muthsam, H. J. 2017, Living Reviews in Computational Astrophysics, 3:1, 159 pages

Kupka, F., Zaussinger, F., & Montgomery, M. H. 2018, MNRAS, 474, 4660

Leitner, P., Lemmerer, B., Hanslmeier, A., et al. 2017, ApSS, 362, 181 (13 pp.)

Lemmerer, B., Hanslmeier, A., Muthsam, H., & Piantschitsch, I. 2017, A&A, 598, A126 (13 pp.)

Magic, Z., Weiss, A., & Asplund, M. 2015, A&A, 573, A89 (17 pp.)

Mundprecht, E., Muthsam, H. J., & Kupka, F. 2013, MNRAS, 435, 3191

Muthsam, H. J., Kupka, F., Löw-Baselli, B., et al. 2010, New Astronomy, 15, 460

Nordlund, Å. 1982, A&A, 107, 1

Nordlund, Å., Stein, R. F., & Asplund, M. 2009, Living Reviews in Solar Physics, 6:2, 117 pages

Rosenthal, C., Christensen-Dalsgaard, J., Nordlund, Å., Stein, R., & Trampedach, R. 1999, A&A, 351, 689

Smalley, B., Antoci, V., Holdsworth, D. L., et al. 2017, MNRAS, 465, 2662

Sonoi, T., Samadi, R., Belkacem, K., et al. 2015, A&A, 583, A112 (11 pp.)

Stein, R. F. 2012, Living Reviews in Solar Physics, 9:4, 51 pages

Stein, R. F. & Nordlund, Å. 2001, ApJ, 546, 585

Tanner, J. D., Basu, S., & Demarque, P. 2016, ApJ, 822, L17 (5 pp.)

Unno, W. & Spiegel, E. A. 1966, PASJ, 18, 85

Yixiao, Z., Asplund, M., & Collet, R. 2019, ApJ, 880, 13 (10 pp.)